

Angolan highlands peatlands: Extent, age and growth dynamics

Mauro Lourenco^{a,b}, Jennifer M. Fitchett^{a,*}, Stephan Woodborne^{c,d}

^aSchool of Geography, Archaeology and Environmental Studies, University of the Witwatersrand, South Africa

^bNational Geographic Okavango Wilderness Project, Wild Bird Trust, South Africa

^ciThemba LABS, Private Bag 11, Wits, South Africa

^dStable Isotope Laboratory, Mammal Research Institute, University of Pretoria, South Africa

*Corresponding author at: Bernard Price Building, University of the Witwatersrand, Private Bag 3, Wits 2050, South Africa. Email: Jennifer.Fitchett@wits.ac.za

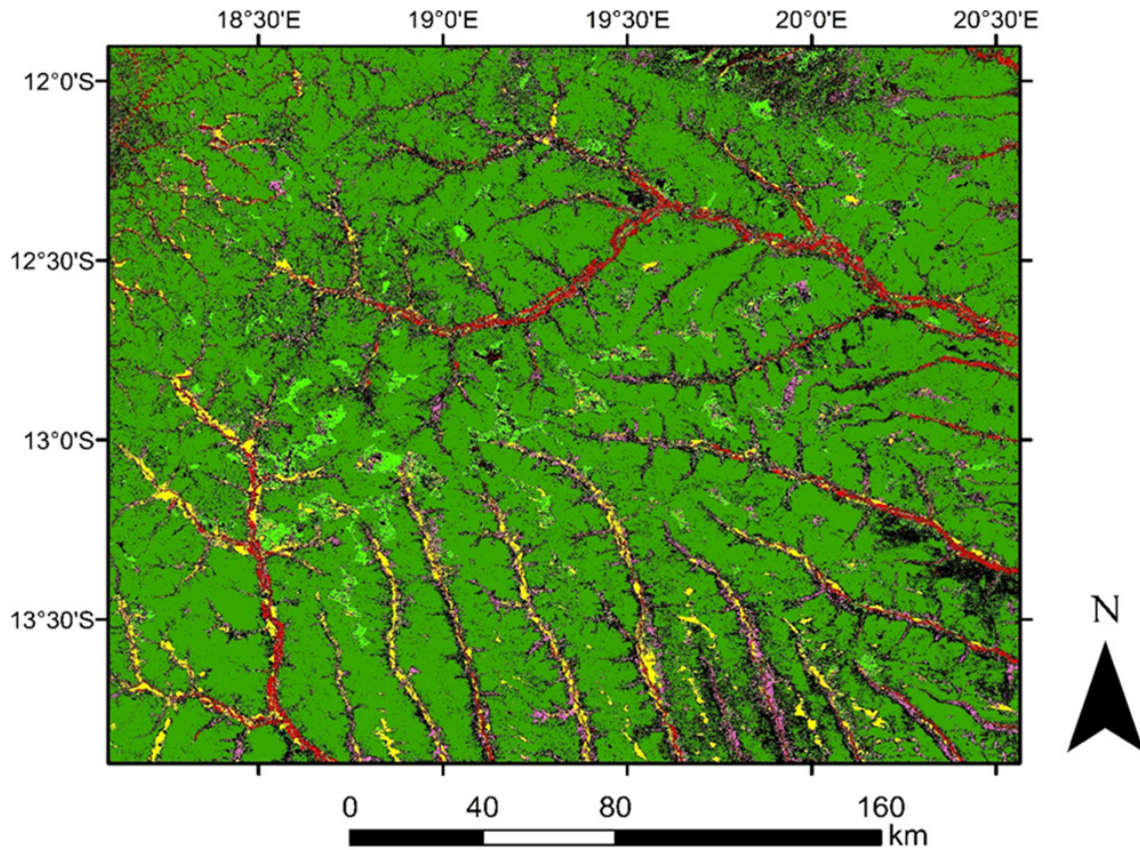
Highlights








- First peatland map in the Angolan Highlands using Google Earth Engine.
- The peatland extent in Angola is much larger than previously estimated.
- The peatlands have formed in lake environments, river floodplains and terraces.
- The African Humid Period could be linked as a driver of peatland initiation.
- These previously unrecognised peatlands are under anthropogenic pressure.

Abstract

The Angolan highlands are hydrologically and ecologically important, supporting peatland deposits. Peatlands are carbon rich ecosystems and are the largest terrestrial carbon store. We present a first estimate of the extent of peatlands in the Angolan Highlands, using Google Earth Engine. Our conservative estimate of peatland coverage is 1634 km², 2.65% of a mapped area spanning approximately 61,590 km². This is a crucial first step in providing the peatland carbon inventory for the region and to facilitate conservation and management strategies. We include the peatland characteristics with respect to topographic data and common remote sensing indices of Normalised Difference Vegetation Index and Normalised Difference Water Index. The results suggest that Angolan Highlands peatland is highly variable in terms of elevation, slope, vegetation cover and standing water occurrence. Radiocarbon dating of riparian peatlands suggest two stages of peatland initiation: one about 7100 cal. yr BP, during the African humid period, and another from about 1100 cal. yr BP to present after the African humid period ended. The temporal control of riparian peat formation is river dynamics and the formation of terraces. Source lake peatland is slightly younger and has average maximum age of 890 cal. yr BP. The Angolan Highlands ecosystem and peatlands are possibly under strain from anthropogenic influence and climate change, making this peatland deposit a potential carbon emission source.

Graphical abstract



Legend	Overlap Landsat 8 and Sentinel 2 classifications	Area km ²
	Peatland	1634
	Miombo woodland	39283
	Valley grassland	164
	Upland grassland	3482
	Water	34
	Cleared/ cultivated land	2299
	Non-overlapping total area	13226

The first map of the Angolan Highlands peatlands. An estimated peatland area of 1632 km² is derived from the overlap of the Landsat 8 and Sentinel 2 random forest classifications

Keywords: Carbon storage; Radiocarbon; Remote sensing; Okavango; Normalised Difference Vegetation Index; Google Earth Engine

1. Introduction

Peatlands are of critical importance, having great economic, ecological, and cultural value (Ramsar, 2002; Limpens et al., 2008; Xu et al., 2018). Peatlands are terrestrial wetland ecosystems, providing a range of ecosystem services as they regulate and filter water flows (Frolking et al., 2011; Evers et al., 2017; DeLancey et al., 2019), aid in agricultural production (Page et al., 2011), are an energy source (Montanarella et al., 2006), and they support biodiversity (Minayeva et al., 2017; Xu et al., 2018). The most important peatland function, that is poorly quantified globally, is ecosystem carbon storage (Rieley and Page, 2016; Xu et al., 2018). Covering 3% of the earth's surface, peatlands are the largest natural terrestrial carbon store (Page et al., 2011), containing more carbon than all the world's forests (Joosten, 2011). Over the last decade, unprecedented growth of fossil fuel emissions and rising global temperatures have placed greater importance on carbon sinks (Friedlingstein et al., 2019; GCP, 2020; Loisel et al., 2021). Accurate mapping of peatlands is essential to determine the extent and carbon pool of peatlands in relation to global carbon stock, and to facilitate peatland preservation (Rieley and Page, 2016; Xu et al., 2018; Minasny et al., 2019).

Global estimates are often based on coarse country inventories and outdated global soil maps (Tanneberger et al., 2017; Xu et al., 2018; Minasny et al., 2019). Estimates of global peatland extent range from 1 to 4.6 million km², and carbon stock estimates range between 113 and 612 Pg carbon (Minasny et al., 2019). The large data ranges have been attributed to the compilation of different estimations from various sources (Joosten, 2010; Page et al., 2011), and the recycling of data without careful consideration to the level of accuracy and the inventory techniques used (Joosten, 2010; Rieley and Page, 2016). To confound matters, there is no globally accepted definition for peat or peatland (Xu et al., 2018; Minasny et al., 2019). Peat is classified as a soil with high organic matter content, which ranges from 30% to 100% depending on the definition used (Joosten and Clarke, 2002; Montanarella et al., 2006; Lindsay, 2010). Peatlands have been defined as having a minimum peat thickness ranging from 10 to 100 cm, subject to local classification schemes or scientific discipline (Bord na Móna, 1984; Joosten and Clarke, 2002; Montanarella et al., 2006; Xu et al., 2018). The high organic matter content results from a combination of peat forming vegetation and incomplete decomposition of organic matter due to waterlogged and anoxic conditions (Montanarella et al., 2006; Lawson et al., 2015).

Most known peatlands in the northern hemisphere have been mapped, covering parts of Europe and North America (Rieley and Page, 2016; Tanneberger et al., 2017). Deposits also occur in the tropics, mostly in Southeast Asia, the Caribbean and Central America, South America, and Africa (Rieley and Page, 2016). Tropical peatlands have been defined as peats that lie between the Tropics of Cancer and Capricorn, including both lowland and upland peat (Page et al., 2007, Page et al., 2011). Africa reflects a diversity of peatland depositional environments that vary between sites and are mostly groundwater fed, reflecting the dry climate of the continent (Grundling and Grootjans, 2016). Large ombrotrophic bogs do exist in wet equatorial regions such as Congo Basin (Davenport et al., 2020). Page et al. (2011) provide an estimate of peatland extent for Angola at 2640 km², a value that was later rereported in Rieley and Page (2016). The estimate was derived from the maximum area of 10,261 km² for histosol estimation in the Global Peatland Database (GPD, 2004), as histosols are regarded as peats in some global peat inventories (Montanarella et al., 2006; Xu et al., 2018). Joosten (2010) provides two estimates for Angolan peatland extent, one for 1990 and one for 2008, at 10,000 km² and 9910 km², respectively. Such estimates are not always

strictly comparable due to different definitions of peat and sampling methods used (Rieley and Page, 2016).

Angola hosts unique habitats and species and is possibly one of the least documented biodiversity hotspot areas in the world (Myers et al., 2000). Exploratory surveys conducted by the National Geographic Okavango Wilderness Project (NGOWP) have identified extensive peat deposits in the eastern Angolan Highlands (Conradie et al., 2016; Goyder et al., 2018). The difficulty in accessibility and the large-scale mapping requirement of the Angolan Highlands means that the carbon inventory of this peatland deposit remains unknown. This study uses Google Earth Engine (GEE), a remote sensing (RS) approach, to map these peatlands. Through background knowledge of the Angolan Highlands, a land cover classification is provided, including a first map of the potential peatland extent. Peatland characteristics with respect to common RS indices such as Normalised Difference Vegetation Index (NDVI), Normalised Difference Water Index (NDWI) and topographic data – elevation and slope are included. Radiocarbon (^{14}C) dates of several peat cores collected from the study site also inform the possible control of peatland formation for the Angolan Highlands.

2. Methods

2.1. Study area

The Angolan Highlands is a central water source region for three major river basins of sub-Saharan Africa, contributing to the Congo basin to the north, the Zambezi basin to the east, and the Okavango basin to the south (Milzow et al., 2009; Abiodun et al., 2019). The highlands are the only source region of the Okavango Delta, an area rich in species diversity (Marazzi et al., 2017; Yurco et al., 2017). Civil war between 1975 and 2002, and widespread minefields have hindered access to the highlands (Conradie et al., 2016; Midgley and Engelbrecht, 2019) for nearly 50 years, and despite its hydrological and ecological significance, it remains little studied. The NGOWP has undertaken the most widespread scientific research in the highlands over the last decade. Since 2012, surveys have highlighted previously undocumented indigenous fauna (Conradie et al., 2016; Taylor et al., 2018) and flora (Goyder et al., 2018).

The Angolan Highlands mapped area for this study is in the southeast of Angola (Fig. 1). The mapped area spanning a latitudinal range of $11^{\circ}54'$ – $13^{\circ}54'$ S and longitudinal range of $18^{\circ}05'$ – $20^{\circ}34'$ E covers approximately 61,590 km², and has an elevation range from 1119 m.asl in the southeast of Moxico province to 1676 m.asl near the Cuito Source Lake. It is part of an extensive interior plateau that covers 65% of the country (Huntley et al., 2019). It is characterised by a vast peneplain draining Kalahari sands, with slow flowing rivers that meander across a gently sloping plateau towards the southeast (Goyder et al., 2018; Huntley et al., 2019). The region has cool annual temperatures of 15 °C and annual rainfall between 900 and 1320 mm, with less rainfall in the south (Abiodun et al., 2019; Huntley et al., 2019). The climate is strongly seasonal, with hot, wet summers from October to May and mild to cool, dry winters from June to September (Abiodun et al., 2019; Huntley et al., 2019).

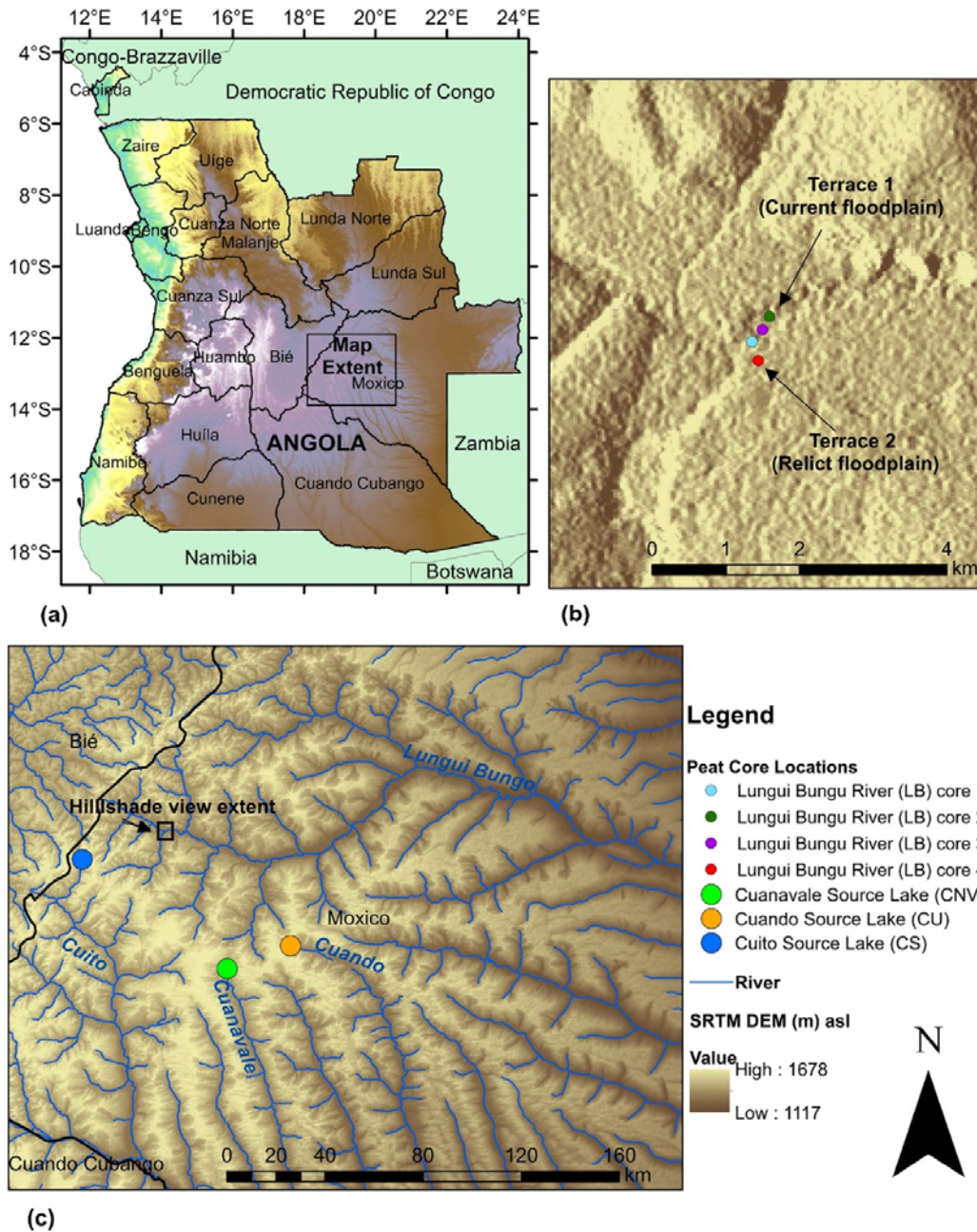


Fig. 1. Study site map, (a) Map extent within Angola, (b) Hillshade view of the four riparian Lungui Bungu River cores; samples 1, 2 and 3 lie within the current river floodplain, terrace 1, and sample 4 lies on the relict floodplain, terrace 2, and (c) Map extent for this study, showing the three remaining peat core locations and the hillshade view extent.

The highlands lie within the Angolan miombo woodland ecoregion and contain tropical and subtropical grasslands, tree, and shrub savannas (Goyder et al., 2018; Huntley et al., 2019). The wide river valleys are characterised by extensive wet grasslands, peatlands, and ox-box lakes (Conradie et al., 2016). The impeded drainage and high precipitation in the rainy season cause temporarily waterlogged soils in the valleys that support humid grassland borders with humic topsoil and dwarf shrubs and prevent the development of miombo woodland (Conradie et al., 2016). The surrounding hills are dominated by miombo woodland (Conradie et al.,

2016; Goyder et al., 2018). Miombo is the Swahili word for oak-like *Brachystegia*, a genus of tree comprising many species (Huntley et al., 2019; WWF, 2021). The miombo woodlands contain over 8500 plant species, they provide habitat for wildlife including the largest populations of elephants in Africa, and support millions of people who are dependent on the woodlands for their livelihoods (WWF, 2021). The NGOWP has extracted seven peat cores from four areas in the Angolan Highlands. Four samples were collected along the Lungui Bungu River, and the remaining three samples were collected from the Cuito, Cuanavale and Cuando source lakes (Fig. 1).

2.2. Peatland mapping

GEE has an extensive catalogue of RS datasets with various spectral and spatial resolutions that have been used for multiple applications, including land cover classifications and wetland mapping (Mahdianpari et al., 2019; Mutanga and Kumar, 2019; Amani et al., 2020). Due to the unique characteristics of peatlands, multisensory mapping approaches are often implemented, using optical, radar and LiDAR satellite imagery to identify and discriminate peatland from other wetland features (Mahdianpari et al., 2019; DeLancey et al., 2019). Satellite image selection is dependent on the characteristics of the peatland for each site (DeLancey et al., 2019; Amani et al., 2020). Although not exclusively, tropical peatlands have been mapped according to distinct features, including vegetation cover, standing water occurrence, and topography (Jaenicke et al., 2008; Draper et al., 2014; Dargie et al., 2017). GEE applications can operate independently, but due to the high geographic variability of peatlands, a level of ground truthing is required to support the GEE application (DeLancey et al., 2019; Mahdianpari et al., 2019).

2.2.1. GEE data exploration

All RS data was acquired, processed, and obtained directly from GEE (Supplementary Material: Table 1). There are no site-specific land cover maps of the area (Fig. 1c). Through exploratory analysis using GEE, the Copernicus Global Land Cover Layers: CGLS_LC100 collection 3 product was used to generate an unsupervised land cover classification (Fig. 2). The product classification has a 100 m resolution and a global accuracy of 80% (Buchhorn et al., 2020). It is used here to provide an overview of the land cover of the highlands. The product maps were produced over the period 2015–2019, spanning the dates of NGOWP field visits.

There are distinct land cover classes in the mapped area; most of the cover is *closed forest, deciduous broad leaf* which is classified in the hills surrounding the river valleys (Fig. 2). The river valleys are classified as *shrubs, herbaceous vegetation, herbaceous wetland* or *cultivated land*. According to the CGLS_LC100 product, the Highlands comprise 176 km² of *herbaceous wetland*, covering 0.29% of the mapped area. 72.70% coverage is *closed forest, deciduous broad leaf*, and 17.12% makes up the combined two *open forest* classes. This default land cover product has limited resolution and land cover classes do not relate specifically to peatlands; hence a supervised classification of the area was generated using GEE.

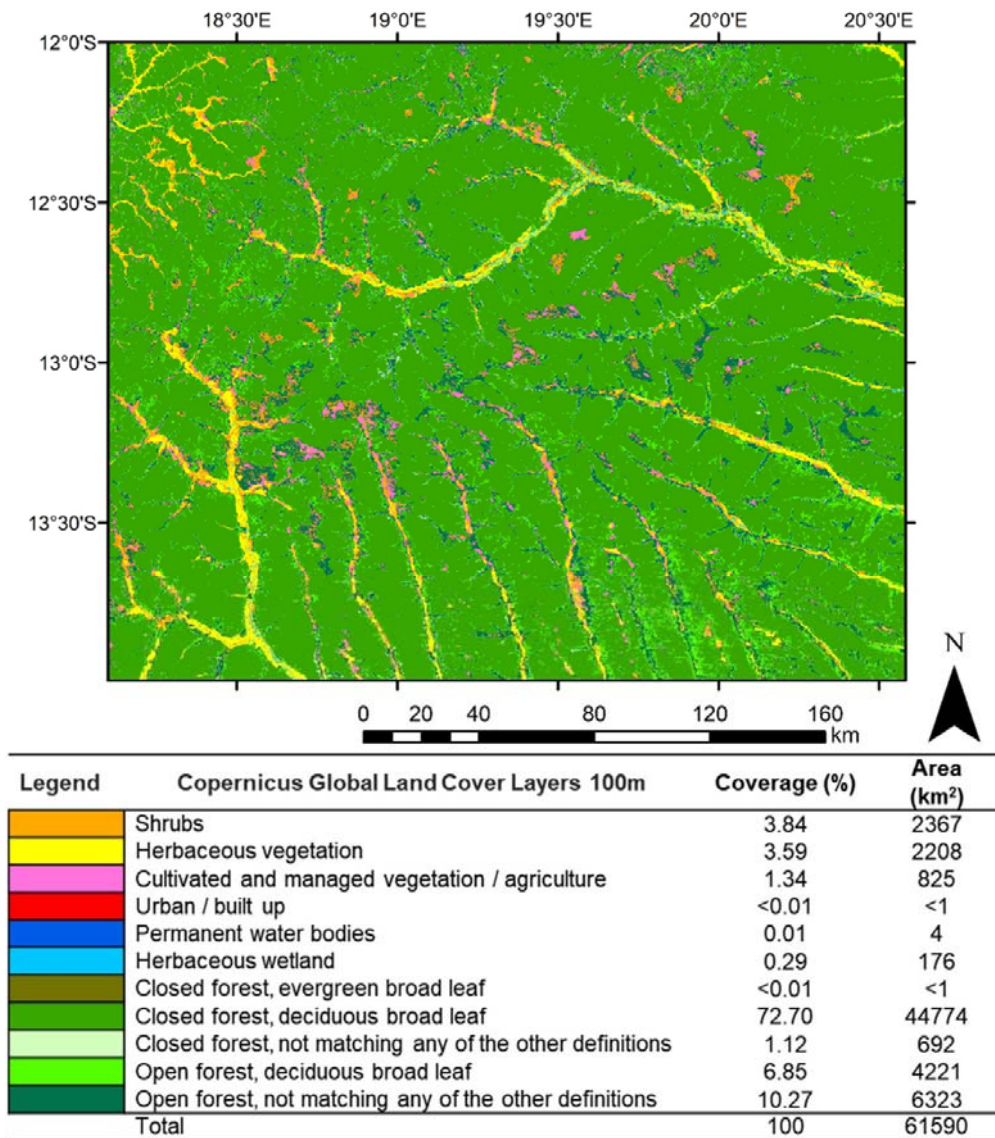


Fig. 2. Copernicus Land cover class area and coverage of the Angolan Highlands.

2.2.2. GEE classification data

USGS Landsat 8 (L8) and Copernicus Sentinel-2 (S2) satellite data were used to generate two separate land cover classifications of the mapped area. Although at different resolutions, these sensors have similar spectral bands and archives (USGS, 2021; ESA, 2021), that span the NGOWP expedition dates. The GEE catalogue stores the USGS L8 Surface Reflectance (SF) Tier 1 dataset and the Copernicus S2 MSI: Multispectral Instrument, Level-2A Surface Reflectance dataset, which are both atmospherically corrected products (USGS, 2021; ESA, 2021). Clouds from both datasets were removed from the image composites by filtering out images with greater than 5% cloud cover.

A random forest (RF) classification was performed on a cloud-free median composite of both the L8 and S2 datasets over the date range 2017-03-28 to 2021-02-14. The starting date corresponds to the S2 product availability on GEE. The L8 RF classification was based on six spectral bands at 30 m resolution, and the S2 RF classification was based on ten spectral bands at 20 m resolution (Supplementary Material: Table 1). RF is a non-parametric classifier and has been shown to outperform other advanced machine learning tools such as Decision Tree (Thanh Noi and Kappas, 2018), is simpler to complete than Support Vector Machine (SVM), as SVM requires modification of many parameters (Rodriguez-Galiano et al., 2012), and is not sensitive to noise and overtraining (Gislason et al., 2006). RF can manipulate high-dimensional RS data and has shown high classification accuracies in various wetland studies (Mahdianpari et al., 2017, Mahdianpari et al., 2019; Whyte et al., 2018).

Six land cover classes were chosen for the classification. These include peatland, miombo woodland, valley grassland, upland grassland, water, and cleared/cultivated land. Identical training and testing polygons were used for both classifications, these object-based polygons were derived from the lower resolution RGB – 30 m optical L8 cloud-free median composite. A total of 75 polygons covering 5.69 km² were drawn on the GEE interface (Supplementary Material: Table 2 and Fig. 1). Polygons were drawn in the centre of distinct features that represented the land cover sites directly observed in the field, this was to reduce edge effect inaccuracies due to the difference in resolution between the two satellites. An object-based classification approach has been shown to be superior to a pixel-based classification for wetland mapping (Mahdianpari et al., 2019). The polygon data were randomly split, 70% used for training and 30% used for testing the classification, the error matrices for each classification were generated on the GEE console.

2.2.3. Validation and accuracy assessment of classifications

For validation purposes overall accuracy, kappa coefficient, producer accuracy, and user accuracy were calculated for each classification using the error matrices (Onojeghuo et al., 2018; Mahdianpari et al., 2019). The McNemar test (McNemar, 1947) was used to determine whether the accuracies of the individual classifications are statistically significant from one another. This non-parametric test is based on the classification confusion matrix which is based on a chi-squared (χ^2) distribution with one degree of freedom and assumes the number of correctly and incorrectly pixels identified pixels are equal for both classification scenarios (Onojeghuo et al., 2018; Mahdianpari et al., 2019). The equation for McNemar's test is:

$$\chi^2 = \frac{(f_{12} - f_{21})^2}{f_{12} + f_{21}} \quad (1)$$

where f_{12} and f_{21} represent the number of pixels that were correctly identified by one classifier as compared to the number of pixels that the other method incorrectly identified, respectively. All statistical analyses were performed using Python 3.8.

2.2.4. Overlap calculation of the two RF classifications

The two independent RF classifications were exported from GEE to ArcMap 10.2 for visualization and layer calculations. The classifications were overlapped on top of one another using the Raster Calculator tool from the spatial analyst toolbox in ArcMap 10.2. An overlap and non-overlap map was generated, including an error matrix of overlap and nonoverlap area between the two RF classifications.

2.2.5. GEE vegetation and water occurrence data

Selected bands from the median L8 and S2 composites that were used in the RF classification were used to generate a NDVI a NDWI composite for each satellite. NDVI is one of the most widely used vegetation indices, describing the greenness, relative density, and health of vegetation (USGS, 2020). NDVI values range from +1.0 to -1.0. Negative values indicate water bodies, while low NDVI values (0.1 or less) indicate barren rock or sand. Sparse vegetation such as shrubs and grasslands may result in moderate NDVI values between 0.2 and 0.5 and high NDVI values between 0.6 and 0.9 correspond to dense vegetation such as forests (USGS, 2020). The equation for NDVI that was used is (Rouse et al., 1974):

$$NDVI = \frac{(Near\ Infrared\ Band - Red\ Band)}{(Near\ Infrared\ Band + Red\ band)} \quad (2)$$

NDWI refers to at least two separate RS derived indices related to liquid water: one defined by McFeeters (1996), is used to monitor changes to water content in water bodies, using the green and Near Infrared (NIR) bands. Another is defined by Gao (1996), which uses the NIR and Shortwave Infrared (SWIR) bands to monitor changes in water content of leaves. This study uses the index as defined by McFeeters (1996), as tropical peatland features have been mapped according to standing water occurrence (Draper et al., 2014; Dargie et al., 2017). NDWI values range from +1.0 to -1.0, the NDWI of Mcfeeters (1996) was used to maximise the typical reflectance of water features, which have positive values, while soil and terrestrial vegetation have zero or negative values (Mcfeeters, 1996). The equation for NDWI that was used is (Mcfeeters, 1996):

$$NDWI = \frac{(Green\ Band - NIR\ Band)}{(Green\ Band + NIR\ band)} \quad (3)$$

2.2.6. GEE topographic data

The 30 m resolution Shuttle Radar Topography Mission (SRTM) digital elevation model (DEM) provided by NASA was used to provide three topographic map layers: elevation, slope and hillshade. Slope represents the angle of the terrain in degrees and hillshade is a 3D representation of the surface, with the sun's relative position used for shading the image (ESRI, 2016). Hillshade is used for illustrative purposes.

2.2.7. Peatland characteristics with reference to NDVI, NDWI and topographical data

The individual L8 and S2 peatland classes from each RF classification were joined to the respective vegetation (NDVI) and standing water occurrence (NDWI) datasets from each respective satellite. The L8 peatland class was joined to the two topographical raster datasets (elevation and slope) as it has the same resolution of 30 m. When joined, distribution plots from the joined data were produced to demonstrate the peatland characteristics with reference to NDVI, NDWI and topographical data.

2.3. Peat core dating methods

2.3.1. Peat core collection and subsampling

Two peat cores were extracted from each sampling site. The cores were collected in two separate NGOWP expeditions, the first made use of a Russian corer to collect the source lake

cores. A Russian corer cuts the core in a horizontal plane, which reduces any mixing of material which occurs during vertical cutting of the core (De Vleeschouwer et al., 2010). The second expedition collected cores in the riparian zone of the Lungui Bungu River by pressing c.120 mm diameter stainless steel tubes vertically into the deposit, thereafter the peat surrounding the core was excavated. In all cases, the peat cores terminated when the equipment entered white sand. For this study, the lowermost section of the peat core is deemed the basal age of the individual core. The source lake cores were refrigerated <4 °C and were subsequently subsampled at 2 cm resolution in the laboratory; in-field subsampling could not be performed in the remote source lake areas. The LB cores were subsampled at 2 cm (LB core 1) and 1 cm (LB cores 2–4) resolution in the field. Cores were removed from the stainless-steel sampling tube and split in half. The outer surfaces were cleaned to minimize any impact of the coring technique. Thereafter each aliquot was carefully sliced from the cleaned core and subsampled for dating analysis.

2.3.2. AMS dating strategy and dating technique

The AMS sampling strategy focused on core top, core base, and one intermediate sample for the CU and each LB core. A high-resolution strategy was implemented for the CS and CNV cores to better resolve additional core data, not reported here. Radiocarbon dating followed standard pre-treatment using acid (HCl), alkali (NaOH), and acid (HCl) followed by extensive washing with deionized water (Brock et al., 2010). Plant rootlets were removed using tweezers. Samples were oven dried and aliquots of the ultra-fine organic component were combusted in evacuated glass tubes with CuO and Ag (Brock et al., 2010). The resulting CO₂ was graphitized before measuring the ¹⁴C content. Radiocarbon dates were calibrated using the Southern Hemisphere SHCal20 model (Hogg et al., 2020). Radiocarbon dating was performed at iThemba Labs, Wits, South Africa. Age-depth models were calculated using the Bayesian BACON approach to age-depth modelling (Blaauw and Christen, 2011).

3. Results

3.1. Random Forest classifications

The individual RF classification maps show distinct separation of all land cover types at the respective resolutions (Fig. 3). Peatlands are generally classified in the river valleys alongside valley grassland and water. The miombo woodland dominates the landscape, upland grasslands are classified as distinct features within the miombo woodland and cleared/cultivated land are classified in areas surrounding the river tributaries and main water courses.

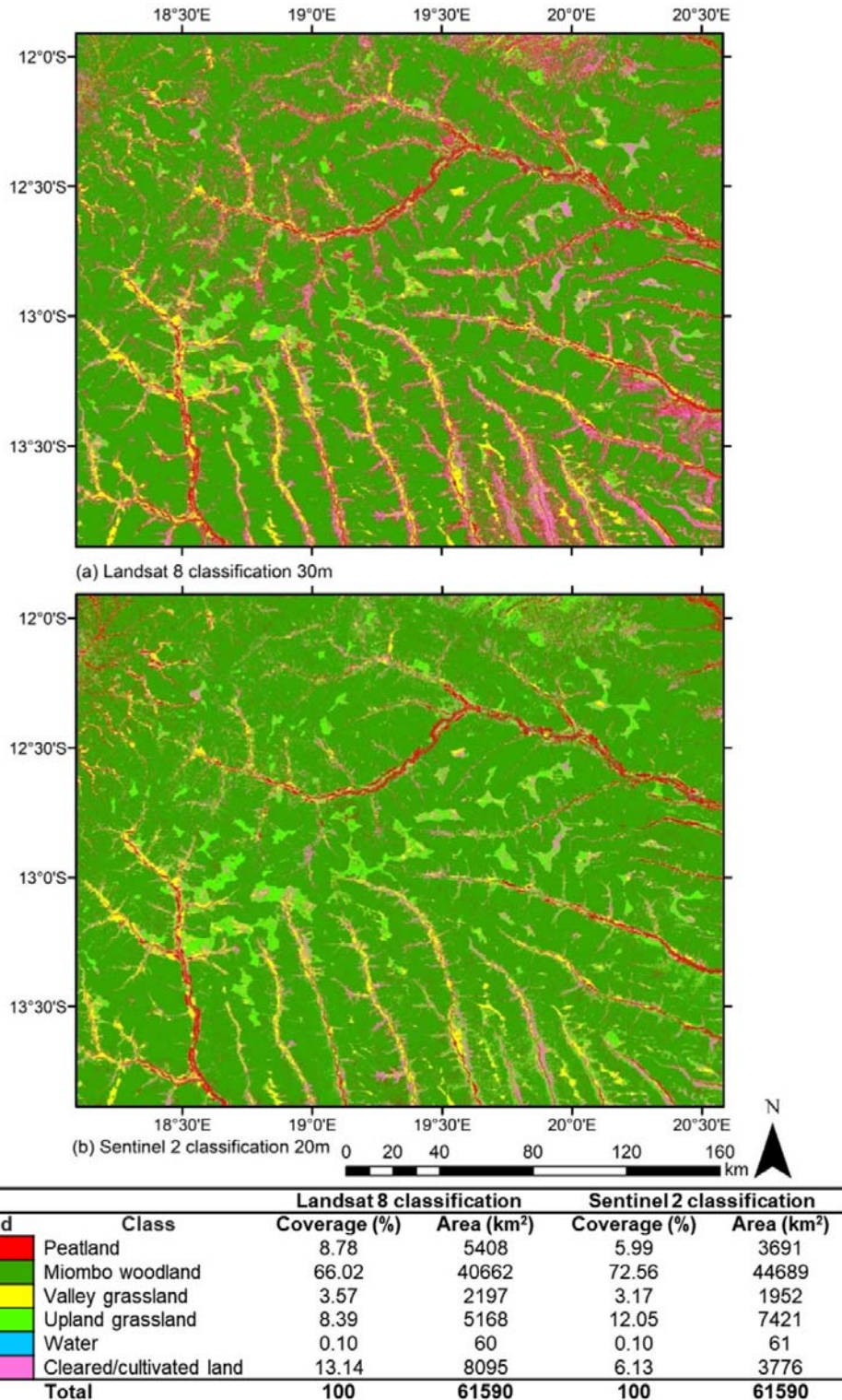
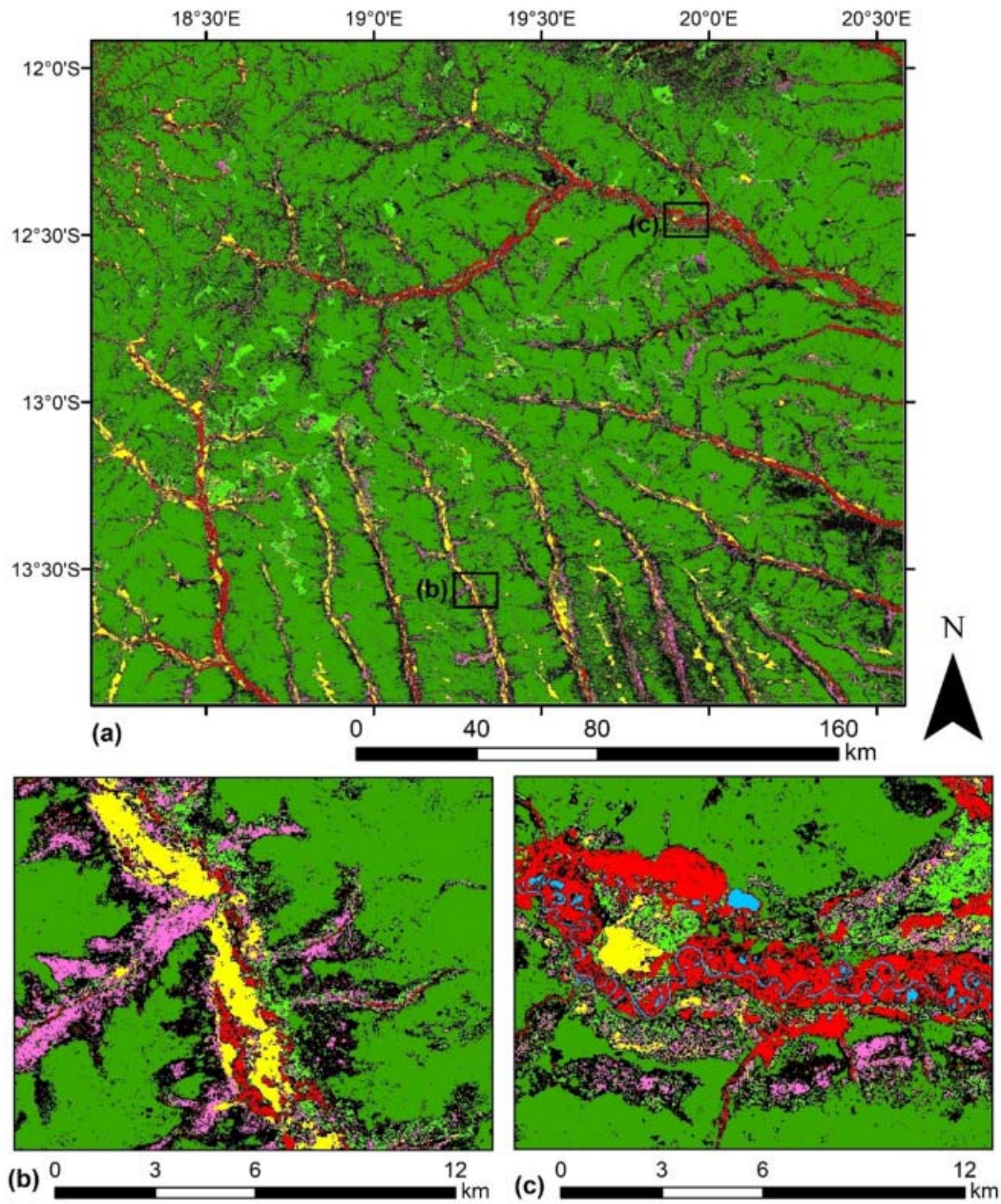


Fig. 3. (a) Landsat 8 and (b) Sentinel 2 RF classifications including coverage and area of each class.



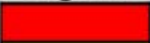






Legend	Overlap Landsat 8 and Sentinel 2 classifications	Area km ²
	Peatland	1634
	Miombo woodland	39283
	Valley grassland	164
	Upland grassland	3482
	Water	34
	Cleared/ cultivated land	2299
	Non-overlapping total area	13226

Fig. 4. (a) Overlap and non-overlap map showing the extent of panel b and c, (b) and (c) are zoomed in sections of the mapped area.

3.2. Accuracy assessment

The accuracy assessment reveals a high overall accuracy of 98.67% and 97.71% for the L8 and S2 RF classifications, respectively (Supplementary Material: Tables 3 and 4). The kappa coefficient values of 0.9836 (L8) and 0.9842 (S2) demonstrate a high level of agreement for each classification. Peatland had a user and producer accuracy >97% for both classifications. The McNemar test revealed that the difference between the accuracies of the L8 and S2 classifications was not statistically significant ($p = 0.9791$, McNemar's test chi-square value = 0.000687). While the accuracies of each classification are not statistically significant from one another, there are spatial and area discrepancies between land cover classes from each classification.

3.3. Spatial and area coverage overlap between the two classifications

An overlap and nonoverlap map of the two classifications was generated (Fig. 4). Overlap classes lie in distinct areas, with 48,363 km² (78.53%) of overlap and 13,266 km² (21.47%) of non-overlap between the two classifications. The majority of nonoverlap occurs in the river tributaries and in the North-east and South-eastern sections of the mapped area. The individual classifications have different resolutions; the edge effect caused by the different resolutions where most of the non-overlapping is shown on the edges of distinct land cover features (Fig. 4b). The overlap of the peatland class along the Lingui Bungu River is demonstrated (Fig. 4c). Peatland occurs on the modern river floodplain, terrace 1 – adjacent to the modern river, and on the relict floodplain, terrace 2 – adjacent to miombo woodland, both grassland classes and cleared/cultivated land (Fig. 4c).

An area calculation matrix of overlap and nonoverlap between each class was calculated (Table 1), the bold values are areas of overlap between the two RF classifications.

Table 1. Land area coverage of overlap and nonoverlap between the two RF classifications.

Overlap area calculations (all values are in km ²)	S2 peatland	S2 miombo woodland	S2 valley grassland	S2 upland grassland	S2 water	S2 cleared/cultivated land	L8 class total	L8 class overlap (%)
L8 peatland	1634	2300	3	1181	21	268	5408	30.22
L8 miombo woodland	998	39,283	1	337	5	39	40,662	96.61
L8 valley grassland	3	3	1631	80	<1	479	2197	74.24
L8 upland grassland	427	543	26	3482	<1	691	5168	67.38
L8 water	23	2	<1	<1	34	<1	60	57.42
L8 cleared/cultivated land	606	2559	291	2340	<1	2299	8095	28.40
S2 class total	3691	44,689	1952	7421	61	3376		
S2 class overlap (%)	44.27	87.90	83.56	46.93	56.20	68.11		

3.4. Peatland extent in the context of Angolan peatland

Three separate peatland estimates – one for each RF classification, and one for the overlap from both RF classifications are provided (Table 1). The overlap map area is reported here as the most conservative estimate of peatland coverage (1634 km²). The mapped area covers just 4.94%, 61,590 km² of the total land area of Angola – 1,246,700 km². Providing the context of this deposit within the country is difficult, as the Angolan peatland estimates originate from studies that considered multiple countries from global and tropical peatland perspectives (Supplementary Material: Table 3).

3.5. Peatland characteristics with reference to NDVI, NDWI and topographic data

From visual inspection, the Optical (RGB), NDVI and NDWI depict the same landscape features. The NASA SRTM topographic data illustrates that river valleys are characterised by low slope angles and low elevation in comparison to the surrounding hills, hillshade is used here for illustrative purposes (Fig. 5).

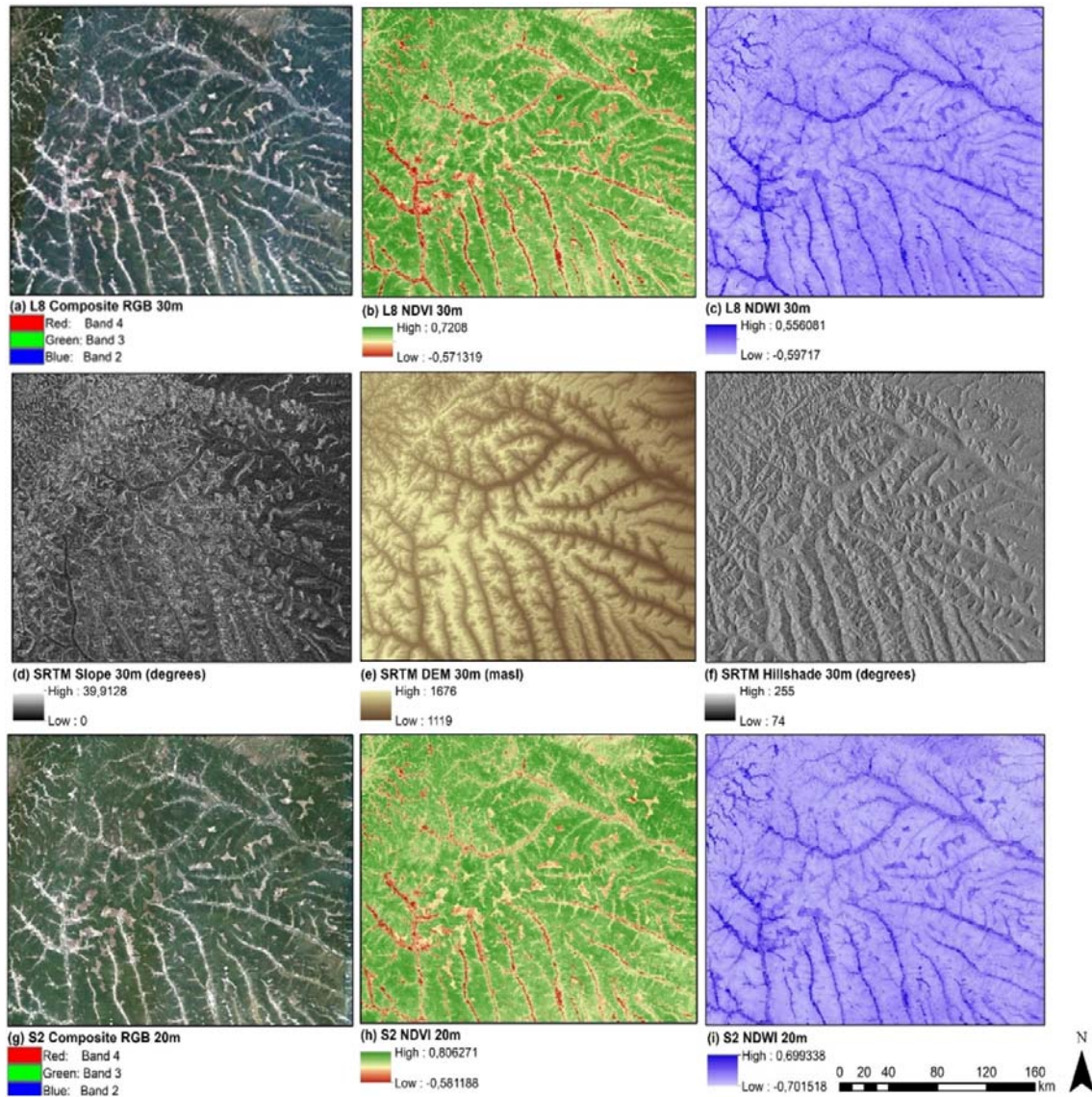


Fig. 5. Optical, vegetation, standing water occurrence and topographic data of the mapped area from Landsat 8 (a–c), NASA SRTM (d–f) and Sentinel-2 (g–i) sensors.

Distribution plots were generated to provide additional peatland characteristics (Fig. 6).

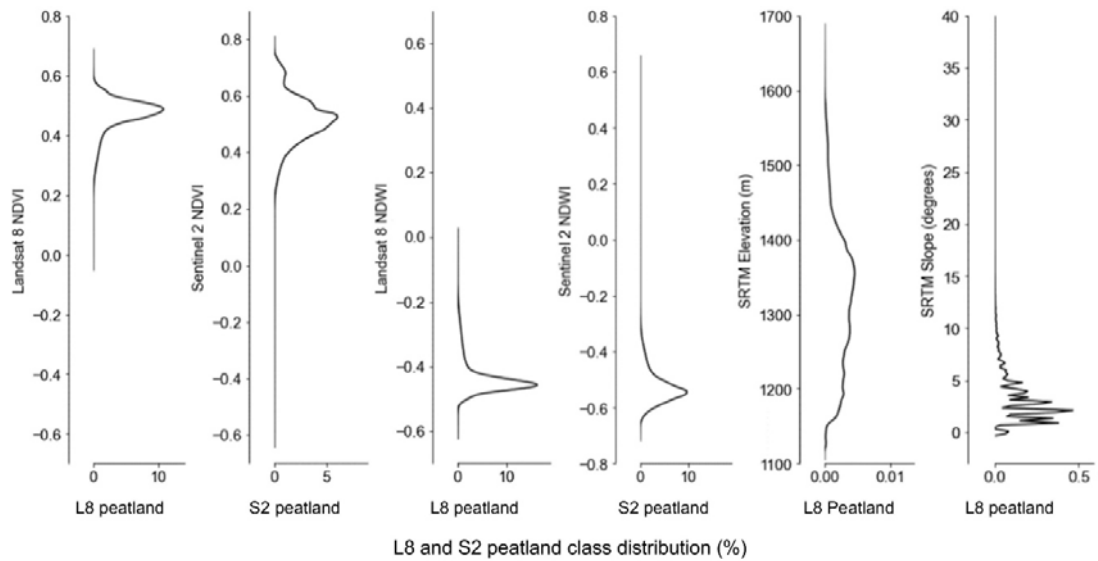


Fig. 6. Distribution plots for L8 and S2 peatland with respect to NDVI, NDWI and SRTM data (elevation and slope). The peaks of each distribution plot show the mode of values for individual peatland pixels. The NDVI and NDWI plots relate to each respective peatland class from each RF classification, the SRTM topographical data relates only to L8 peatland. See Supplementary Material Figs. 2–7 for distribution plots of all landcover classes.

For L8 NDVI, the peatland class has a range of values from -0.04 to 0.68 , an average of 0.47 and mode of 0.48 . For S2 NDVI, the peatland class has a similarly shaped distribution plot to that of L8 peatland class, the range is from -0.63 to 0.80 , an average of 0.51 and mode of 0.5 . For L8 NDWI, the peatland class has a minimum value of -0.62 , average of -0.43 and mode of -0.45 and a positive maximum value of 0.02 . For S2 NDWI, the peatland class is similarly shaped to that of L8 peatland class and L8 NDWI. The S2 peatland class has a large NDWI range from -0.71 to 0.65 and has an average NDWI of -0.53 and peak of -0.5 . For SRTM elevation, the L8 peatland class distribution reveals multiple, wide ranging peaks in comparison to the NDVI and NDWI data that had either one or two peaks, that are much thinner. The average elevation for the L8 peatland class is 1316 m.asl, and has three peaks at 1350 m.asl, 1275 m.asl and 1190 m.asl. For SRTM slope, L8 peatland class has multiple peaks between 0° and 5° , a maximum slope of 40° , and an average of 3.36° .

3.6. Radiocarbon chronology

Each of the Lungui Bungu River peat chronologies shows reasonable age-depth profiles, except for LB core 2 where there is no possible age depth profile due to inversions (Fig. 7e). The LB core 2 sample was collected near an abandoned intensive peat agriculture field, and turbation of this site is evident in Google Earth imagery spanning several years. It is possible that the age inversion is the result of past agricultural working of the peat, although this should be expected for the upper layers, not at depth where the inversion occurs. The age models for cores 1, 3 and 4 suggest that these peat deposits started to grow about 1200 years ago, 1600 years ago, and 7100 years ago respectively. They also indicate that all the cores (including core 2) are still actively growing.

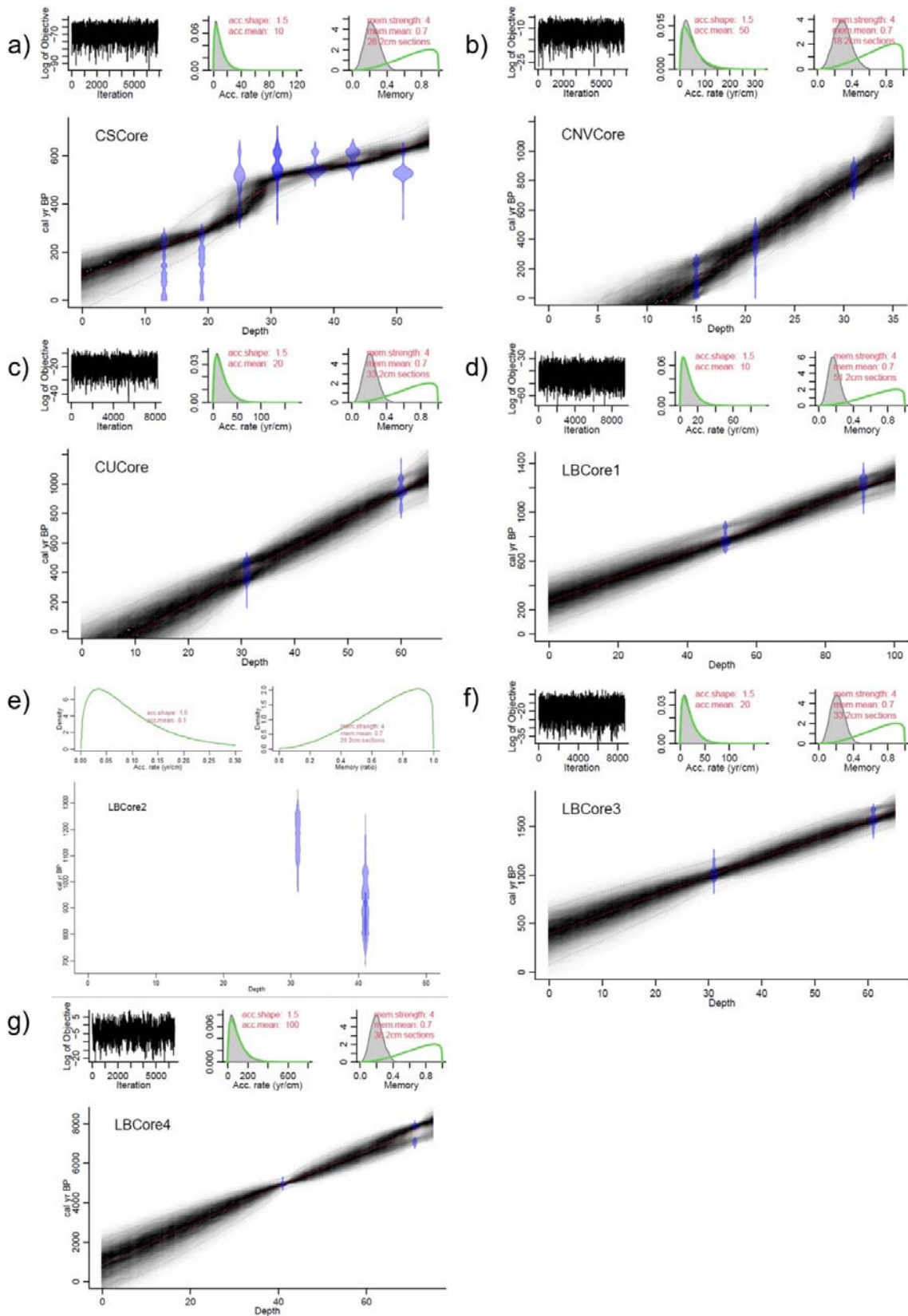


Fig. 7. Bacon Age-depth profiles for Angolan Highlands peat cores, panels a–c represent the age models for CNV: Cuanavale source lake peat, CS: Cuito source lake peat and CU: Cuando source lake cores, respectively. Panels d–g represent the age models for Lungui Bungu River cores 1 to 4, respectively.

The age depth profile of the source lake cores suggests that the CNV core accumulated over the last 800 years, and the CU core accumulated over the last 1000 years. The pattern in the calibrated dates for the CS core indicate very rapid accumulation of approximately half the core, with all material dated below 25 cm having the same age. Between 25 and 19 cm depth there is a substantial jump in the age. This may be a single contaminated date (reject the date for 19 cm) in which case the upper half of the peat may have accumulated at a more gradual pace after the initial rapid growth. Alternatively, the date at 19 cm may be correct (there is no reason to reject it) suggesting slow growth of the peat for 200 years after the initial rapid growth, followed by intermediate growth in the last 200 years. All lake deposits are still actively growing. See Supplementary Material Table 6 for extended AMS dating results.

4. Discussion

4.1. Peatland extent

This study is the first to estimate and map the extent of the peatlands in the Angolan Highlands. The extent of peatlands in Angola is much larger than previously quoted from global studies, which has implications for national carbon budgets. Rieley and Page (2016) is the only study that mentions significant peatland deposits in Angola (Goyder et al., 2018). Rieley and Page (2016) mention that according to Bord na Móna (1984) and Shier (1985), there are extensive deposits in the valley of the River Cuanza, South-east of Catate, about 50 km from Luanda. Luanda is a coastal city that is over 600 km from the Angolan Highlands, meaning that the deposits mapped here have been overlooked (Goyder et al., 2018).

The estimate of 2640 km² from Page et al. (2011) was derived from the maximum estimate of histosols (10,261 km²) minus the shallow histosols and organic soils (7621 km²) from the GPD (2004). The maximum for histosols from GPD (2004) is similar to the estimates of Joosten (2010) for 1990–10,000km² and 2008–9910km² where the 2008 estimate had a 0.90% reduction in area following expected peatland degradation over time (Joosten, 2010). These country estimates do not contain specific reference maps or location details that may be used to link them to the Angolan Highlands. Similarly, this estimate is specifically for the Angolan Highlands and cannot be extrapolated over the entire country. With no clear mention of the Angolan Highlands, it is likely that the estimate from this study is an addition to the best estimate (2640 km²) reported by Page et al. (2011), meaning that the country estimate may be larger (>4274 km²). The Highlands deposit would account for over half (61.90%) of the total peatland of Angola.

PEATMAP is one of the most recent estimates of global peatland extent: cataloguing 4,232,369 km² globally of which the African continent contributes 187,061 km² (Xu et al., 2018). This estimate is an addition to the African and tropical peatland extent. The headwaters of the Angolan Highlands contribute to the largest tropical peatland deposit to the north (Dargie et al., 2017); peatlands have also been identified to the south in the Okavango Delta (Grundling and Grootjans, 2016; Goyder et al., 2018); and there may be potential for further peatland mapping of the Zambezi basin to the east. Considering that the mapped area comprises only 4.94% of the country and approximately 16% of the Angolan highlands, it is likely that there may be more tropical peatland deposits to discover (Lawson et al., 2015), in the Angolan Highlands and surrounding basins.

This study provides a land cover classification of approximately 61,590 km² of the Angolan Highlands. The supervised L8 and S2 RF classifications demonstrate the benefit of field-based knowledge in comparison to a Copernicus global classification product, which returned 176 km² of *herbaceous wetland*. The critical landcover class ‘peat’ or ‘peatland’ is not available in this or any other product on GEE (GEE Data Catalogue, 2021). This is because peatland cannot be detected directly by RS on a global scale as the variety of peatland vegetation and depositional environments is too broad to assess peatland presence based only on surface landscape characteristics (Joosten, 2010; Xu et al., 2018; Minasny et al., 2019). As shown, regional mapping is achievable (Joosten, 2010), the kappa coefficient of each classification is >0.98, interpreted as having perfect agreement (Landis and Koch, 1977).

The overlap map area is reported as the most conservative estimate of peatland coverage (1634 km²). This estimate is where peatland has been classified in both approaches. In each, the peatland class had over 97% producer and user accuracy. Reporting either S2 or L8 peatland coverage would likely overestimate the peatland coverage as only 30.22% of L8 peatland overlaps S2 peatland, and 44.27% of S2 peatland overlaps L8 peatland. The object-based training and testing polygons were identical for both RF classifications, and the differences between the accuracy of the classifications was not statistically significant ($p < 0.05$). It should be noted that these RF classifications are specific to the study site and are user driven.

The differences between each RF classification can be explained by bootstrap aggregation – decision trees are sensitive to the data they are trained on, and small changes in the training set can result in significantly different tree structures (Gislason et al., 2006; Lee et al., 2020). RF takes advantage of this by allowing each individual tree to randomly sample from the dataset with replacement, resulting in different trees, known as bagging (Lee et al., 2020). With respect to feature randomness, RF only picks from a random subset of features, which forces more variation among the trees in the model and ultimately results in lower correlation across trees and more diversification (Gislason et al., 2006; Lee et al., 2020). The result is that with RF, trees are not only trained on different sets of data, but also use different features to make decisions (Gislason et al., 2006; Lee et al., 2020). Furthermore, the difference between the classifications can be explained by the number of bands – L8 used six spectral bands and S2 used ten spectral bands. The additional four Red Edge bands of S2 have been shown to produce better and comparable results to L8 and other S2 bands, respectively (Forkuor et al., 2018). The edge effect inaccuracies brought on by the difference in resolution between each classification is also responsible for some of the non-overlap between the two classifications.

The L8 and S2 classifications predict that peatland exists within the source lake and river valley environments, as was observed in field expeditions. With respect to the peatland class, most of the disagreement between the classifications occurs with the land cover classes of miombo woodland, upland grassland, and cleared/cultivated land. The disagreement between peatland and cleared/cultivated land can be expected as local communities target peatlands and riparian zones for cultivation, as observed at the LB core 2 location. Between the two classifications, peatland is often predicted in small, localised deposits within both the miombo woodland and upland grassland environments. These localised deposits of predicted peatland, away from the source lake and river environments, require further investigation in future field expeditions. In contrast, there is little disagreement with peatland and the valley grassland and water classes, these two classes both exist within the source lake and river valley environments.

4.2. Peatland in relation to NDVI, NDWI and topography

RS classification studies can be used either to identify peatland as a distinct land use (this study) or be used to identify vegetation communities and topographic features within a peatland environment (Lees et al., 2018; Oon et al., 2019). The NDVI, NDWI and topographical data were included to provide further details regarding this peatland deposit.

The NDVI for the peatland class had average of 0.47 and 0.51 for L8 and S2 classes respectively, with distinct peaks (modes) at 0.5, values typical of grassland and shrub vegetation (USGS, 2020). Comparable NDVI values for tropical peatlands are seldom reported. The NDVI of actively growing peatlands is specific to the region and season, reflecting the typical vegetation type growing on the deposit (Šimanauskienė et al., 2019). A total of 115 plant species were identified in the wetland habitat of the Cuito catchment alone (Goyder et al., 2018), 94 of which are associated with peat soils. This high variation of vegetation cover is reflected in the large range in NDVI associated with these peatland deposits. The NDVI values reported here are obtained from a cloud-free median RGB composite of both the L8 and S2 datasets over the date range 2017-03-28 to 2021-02-14, and therefore do not reflect the peatland growing season or growth under a changing climate. To ensure preservation of the Angolan Highlands peatland deposit, future investigation may focus on producing NDVI time-series, including seasonal variation in peatland vegetation coverage. NDVI is a good measure of photosynthetic activity and could be used to estimate peatland productivity (Wang et al., 2004; Boelman et al., 2003, Boelman et al., 2005).

The NDWI for peatland had an average of -0.43 and -0.53 , with distinct modes at -0.45 and -0.5 for L8 and S2 classes respectively, values indicative of terrestrial vegetation growth and not standing water (Mcfeeters, 1996). The NDWI for L8 peat has a maximum value of 0.02, whereas the S2 peat has a maximum value of 0.65 – which is typical of standing water (Mcfeeters, 1996). Although used as a predictor (Delancey et al., 2019), NDWI values for peatlands are rarely reported. The S2 RF classification is demonstrably more sensitive for both the vegetation (NDVI) and water (NDWI) indices over the L8 RF classification, shown by the larger range in each distribution plot. As with the NDVI data, similarly the NDWI plots do not reflect the peatland growing season through time. NDWI is a strong predictor of water table position (Kalacska et al., 2018), making it sensitive to peatland surface water depth (Zhang et al., 2014). Future investigation may focus on producing NDWI time-series, with particular emphasis on water table depth, hydrology, and precipitation.

The Angolan highlands peatland had a maximum elevation of 1676 m.asl, on average the peats are 1316 m.asl and the distribution plots had distinct peaks (modes) at 1350 m.asl, 1275 m.asl and 1190 m.asl. The shape of the density distribution curve of the L8 peatland class is most similar to the L8 valley grassland and cleared/cultivated land classes (Supplementary material: Fig. 6). These classes lie adjacent to one another within the river valleys, which suggest that the control on peat formation is strongly linked to geomorphology. Most of the peatland lies between elevations of 1150 m.asl and 1450 m.asl, and peat formation in upland valleys such as those in the Angolan Highlands also occur in Rwanda (2100 m.asl: Hategekimana and Twarabamenya, 2007), Lesotho (2400 m.asl: Trettin et al., 2008), and Burundi (1500 m.asl: Pajunen, 1996). In these high-altitude regions, the conditions for peat formation are similar to temperate regions (Andriessse, 1988; Page et al., 2011).

The slope distribution plots reveal that most of the peatland landscape is flat as most peaks occur between slope angles of 0–5°, with an average slope of 3.36°. Slope angles of up to 40° suggest that these peatlands are not limited to flat topographies, although this requires direct field measurement. Along the Lungui Bungu river, field observations of peat on steep slopes are associated with the incision of terrace 1 from terrace 2. Denoted by ¹⁴C dates, before terrace 1 existed, the river was dominated by terrace 2, and the incision increased the local gradient (Fig. 8). In some cases, the incision is a cliff face which suggests that maximum slope values are most likely as a response to the local relief driven by the geomorphology of the area.

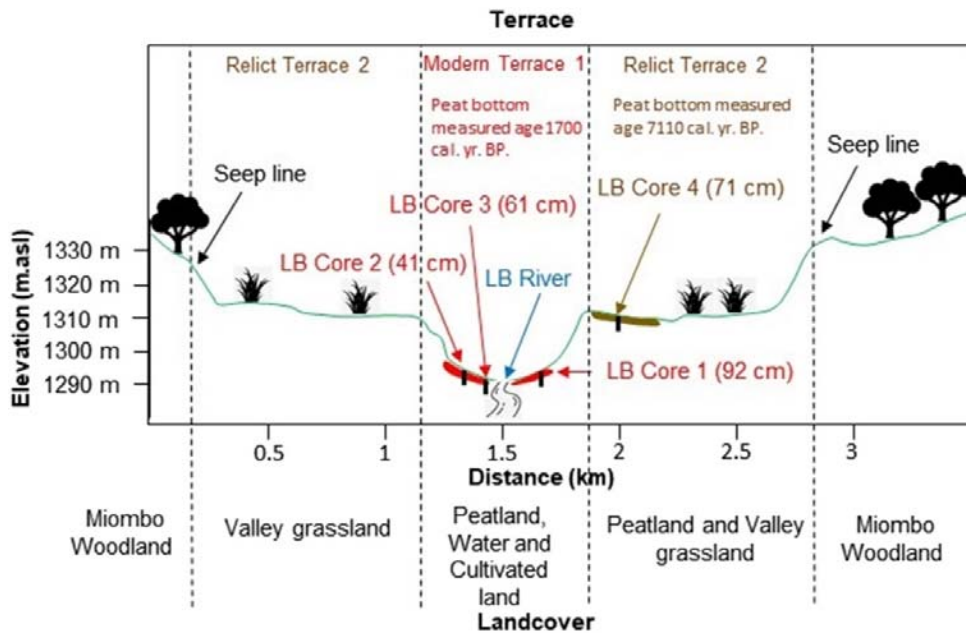


Fig. 8. Cross-section of the peat core sampling site at the Lungui Bungu River.

4.3. Onset of peat formation, potential carbon storage and peatland threats

The highland peatlands are diverse in that they are forming in lacustrine environments, on the current river floodplain and on relict river terraces. These peatlands are minerotrophic; with evidence from field observations and optical imagery, a distinct seep-line exists parallel to higher ground immediately adjacent to the peatlands. This seep-line is the inflow area of ground water, peatland only persists on terrace 2 where there are physical features that pond this water. These are low lying areas of terrace 2 and is why terrace 2 peatland is often patchy and associated with valley grassland and cleared/cultivated land. The valleys are a gentle V-shape, the peatlands all contour downwards towards the river. Effectively the peatlands are the upstream/downstream gradient of the river as they limit river flow. The headwater lakes are areas where steep hillside collapses block the river flow, and they form a lake with the same water supply as the river itself.

The maximum ages of the riparian Lungui Bungu River cores should not be seen as coincidental. The three cores from the current river floodplain, terrace 1, all have basal ages over 1100 years cal. BP while core 4 on terrace 2, has a distinctly different basal date of over 7100 years cal. BP. The age of 7100 years cal. BP may be linked with peat initiation and carbon accumulation related to the African humid period between ~11,000 and

~8000 years cal. BP (Schefuß et al., 2005; Shanahan et al., 2015). The dates are also comparable to those collected in the Central Congo Basin where the Cuvette Central swamp peats returned ages ranging from 10,554 to 7137 years cal. BP (Dargie et al., 2017). Ages of around 1100 years on terrace 1 indicate that the peat has continued to grow since the end of the African humid period at ~3000 years cal. BP (Schefuß et al., 2005; Shanahan et al., 2015) in the Lungui Bungu River.

Along the Lungui Bungu River sampling site, the peat formation on the modern riverbank (terrace 1) is almost ubiquitous, having a greater coverage than terrace 2, where only relict peat patches remain. Local farming practices target terrace 2 peat because it is easily drained. However, drainage also occurs on terrace 1, leading to oxidation and changes to the hydrological buffering that these peats offer. The terrace 1 peats are a control valve between ground water flow and the river, a highly important ecosystem service. Continued peat drainage also potentially destabilises the riverbank. The reduction in peat area on both terraces 1 and 2 may imply that the dynamics of peat in the Lungui Bungu River is a net source of atmospheric carbon rather than a sink on geological time. The age and dynamics of these terrace peats is therefore of considerable interest and warrant future investigation.

The ^{14}C dates reveal that the source lake cores are slightly younger (average basal age of 890 years cal. BP) than the riparian LB cores. The results from the CNV and CU cores suggest slow onset of peat growth that accelerates through time – acknowledging that the evidence for this in CU is based on only two dates. In contrast, the CS core shows extremely rapid peat growth initially, followed by a possible hiatus in growth. The rate of peat formation in the upper part of the CS core is consistent with the rapid rates seen in the CNV and CU cores. The mechanism that underlies the age profile for the CS core is not clear. It could be explained by a catastrophic erosion event, two pulses of growth, changes to climate or possible peat loss due to anthropogenic disturbance.

The average depth of the cores collected for this study is 63.6 cm, Goyder et al. (2018) – part of the NGOWP mention that they directly measured peat to a depth of at least 5 m at the Cuito Source Lake. AMS ^{14}C dating reveals that these peatlands continue to grow but have formed over the last few thousand years. The implications are that the deposit may store significant amounts of carbon (Goyder et al., 2018), and that these deposits have the potential to be an important part of the global carbon economy. This map is the first step in providing the carbon store and serves to promote preservation of the deposit. Future research specific to this study would require a complete ground field survey to verify the land cover classifications, with particular emphasis on peatland extent. In addition, to provide estimates of the carbon inventory, peat depth and bulk density are required.

The threats to the Angolan Highland peatlands and landscape can be linked to anthropogenic practices such as extensive fires, wood and peat fuel extraction, tree clearing, wetland drainage and overgrazing (Conradie et al., 2016; Taylor et al., 2018). Continued population growth, lack of financial means, subsistence agriculture and human pressure on the land are increasing in unprotected, rural areas of Angola (Catarino et al., 2020). These peatlands are highly susceptible to fire and slash and burn agriculture (Conradie et al., 2016; Taylor et al., 2018). The largest burnt areas in rural parts of Angola were recorded between 2003 and 2005, which is linked to the end of the civil war in 2002 (Catarino et al., 2020). During the war, there was emigration from rural communities to urban areas and agricultural fields were abandoned, and when the war ended some displaced people returned and started clearing land for agriculture (Catarino et al., 2020). In contrast, some protected areas of Angola exhibited

decreasing trends in burning during that same period (Catarino et al., 2020). The role of fires and peatland degradation is well documented in the extensive tropical peatlands of South-east Asia (Rieley and Page, 2016; Page et al., 2007, Page et al., 2011), highlighting the need to protect this deposit from the same process.

Angola is particularly vulnerable to climate change, with Regional Climate Models (RCMs) predicting consistent results of an increase of up to 4.9 °C by 2100 and increasing frequency and intensity of droughts for the twenty-first century (Carvalho et al., 2017). The semiarid and subhumid areas will be affected by a shift towards a drier regime (Carvalho et al., 2017), affecting peatland functioning and putting increased strain on rural communities that rely on peatlands for agriculture, water, and fuel (Grundling and Grootjans, 2016). Estimates in 2010 indicated that 10–15% of African peatlands are degraded, releasing 4.3% of global peat CO₂ (Joosten, 2010). These have likely increased. Future conditions associated with a combination of anthropogenic influence and climate change are expected to further increase carbon emissions owing to peatland degradation (Xu et al., 2018; Minasny et al., 2019).

5. Conclusion

The first land cover classification of the Angolan Highlands study area was produced using GEE. This classification includes a conservative area extent of peatland coverage, 1634 km². This is a crucial first step in providing the peatland carbon inventory and to facilitate conservation priorities and management strategies for the area and its surrounding basins, basins that are likely to contain additional unmapped peatland deposits. The relationship between peatland and vegetation cover, standing water occurrence and topographic data was included to further describe these peatlands. Radiocarbon dating of peatland cores informs the possible onset of peatland accumulation for the highlands and has uncovered additional questions about how they have formed and continue to grow. We emphasise that future research in this region is required to focus not only on peatland extent, but also investigate the peatland growth, vegetation, water, and carbon dynamics of this unique environment. Peatlands are extremely important ecosystems that globally, are under threat from anthropogenic influence and climate change, these peatlands are no different and have the potential to have net carbon emissions in future if they remain unprotected.

Funding

Jennifer Fitchett receives funding from the DSI-NRF Centre of Excellence for Palaeosciences.

CRedit authorship contribution statement

Mauro Lourenco: Conceptualization, Methodology, Validation, Formal analysis, Investigation, Data curation, Writing – original draft, Visualization, Funding acquisition.

Jennifer M. Fitchett: Conceptualization, Methodology, Validation, Formal analysis, Investigation, Writing – review & editing, Supervision, Project administration, Funding acquisition. **Stephan Woodborne:** Conceptualization, Methodology, Validation, Formal analysis, Investigation, Resources, Data curation, Writing – review & editing, Visualization, Supervision, Project administration, Funding acquisition.

Declaration of competing interest

The authors declare that they have no known competing financial interests or personal relationships that could have appeared to influence the work reported in this paper.

Acknowledgments

National Geographic Okavango Wilderness Project and Wild Bird Trust exhibition teams are acknowledged for sample collection. Dr. Rainer von Brandis and Götz Neef are acknowledged for discussions and feedback throughout the writing process. iThemba LABS is acknowledged for the radiocarbon dating. Jono Julyan is acknowledged for his assistance with the distribution plots. Dr. David Goyder is acknowledged for his assistance regarding the number of plant species associated with peat soils.

References

- Abiodun, B.J., Makhanya, N., Petja, B., Abatan, A.A., Oguntunde, P.G., 2019. Future projection of droughts over major river basins in Southern Africa at specific global warming levels. *Theor. Appl. Climatol.* 137 (3), 1785–1799.
- Amani, M., Ghorbanian, A., Ahmadi, S.A., Kakooei, M., Moghimi, A., Mirmazloumi, S.M., et al., 2020. Google Earth Engine cloud computing platform for remote sensing big data applications: a comprehensive review. *IEEE J. Sel. Top. Appl. Earth Obs. Remote Sens.* 13, 5326–5350.
- Andriessse, J.P., 1988. *Nature and Management of Tropical Peat Soils. FAO Soils Bulletin 59.* Food and Agriculture Organisation of the United Nations, Rome.
- Blaauw, M., Christen, J.A., 2011. Flexible paleoclimate age-depth models using an autoregressive gamma process. *Bayesian Anal.* 6 (3), 457–474.
- Boelman, N.T., Stieglitz, M., Rueth, H.M., Sommerkorn, M., Griffin, K.L., Shaver, G.R., Gamon, J.A., 2003. Response of NDVI, biomass, and ecosystem gas exchange to long-term warming and fertilization in wet sedge tundra. *Oecologia* 135 (3), 414–421.
- Boelman, N.T., Stieglitz, M., Griffin, K.L., Shaver, G.R., 2005. Inter-annual variability of NDVI in response to long-term warming and fertilization in wet sedge and tussock tundra. *Oecologia* 1;143 (4), 588–597.
- Bord na Móna, 1984. *Fuel Peat in Developing Countries. World Bank Technical Paper No. 41.* The World Bank, Washington, DC.
- Brock, F., Higham, T., Ditchfield, P., Ramsey, C.B., 2010. Current pretreatment methods for AMS radiocarbon dating at the Oxford Radiocarbon Accelerator Unit (ORAU). *Radiocarbon* 52 (1), 103–112.
- Buchhorn, M., Lesiv, M., Tsendbazar, N.E., Herold, M., Bertels, L., Smets, B., 2020. Copernicus global land cover layers—collection 2. *Remote Sens.* 12 (6), 1044.

- Carvalho, S.C., Santos, F.D., Pulquério, M., 2017. Climate change scenarios for Angola: an analysis of precipitation and temperature projections using four RCMs. *Int. J. Climatol.* 37 (8), 3398–3412.
- Catarino, S., Romeiras, M.M., Figueira, R., Aubard, V., Silva, J., Pereira, J., 2020. Spatial and temporal trends of burnt area in Angola: implications for natural vegetation and protected area management. *Diversity* 12 (8), 307–329.
- Conradie, W., Bills, R., Branch, W.R., 2016. The herpetofauna of the Cubango, Cuito, and lower Cuando river catchments of south-eastern Angola. *Amphib. Reptile Conserv.* 10 (2), 6–36.
- Dargie, G.C., Lewis, S.L., Lawson, I.T., Mitchard, E.T., Page, S.E., Bocko, Y.E., Ifo, S.A., 2017. ge, extent and carbon storage of the central Congo Basin peatland complex. *Nature* 542 (7639), 86–90.
- Davenport, I.J., McNicol, I., Mitchard, E.T., Dargie, G., Suspense, I., Milongo, B., Bocko, Y.E., Hawthorne, D., Lawson, I., Baird, A.J., Page, S.S., 2020. First evidence of peat domes in the Congo Basin using LiDAR from a fixed-wing drone. *Remote Sens.* 12 (14), 2196–2209.
- De Vleeschouwer, F., Chambers, F.M., Swindles, G.T., 2010. Coring and sub-sampling of peatlands for palaeoenvironmental research. *Mires Peat* 7.
- DeLancey, E.R., Kariyeva, J., Bried, J.T., Hird, J.N., 2019. Large-scale probabilistic identification of boreal peatlands using Google Earth Engine, open-access satellite data, and machine learning. *Plos One* 14 (6), e0218165.
- Draper, F.C., Roucoux, K.H., Lawson, I.T., Mitchard, E.T., Coronado, E.N., Lähteenoja, O., et al., 2014. The distribution and amount of carbon in the largest peatland complex in Amazonia. *Environ. Res. Lett.* 9 (12), 124017.
- Environmental Systems Research Institute, 2016. *Hillshade function*. Available from <https://desktop.arcgis.com/en/arcmap/10.3/manage-data/raster-and-images/hillshade-function.htm#:~:text=A%20hillshade%20is%20a%20grayscale,to%20specify%20the%20sun's%20position>. (Accessed 30 January 2021).
- European Space Agency, 2021. *Sentinel Level 2A product types*. Available at <https://sentinel.esa.int/web/sentinel/user-guides/sentinel-2-msi/product-types/level-2a>. (Accessed 16 January 2020).
- Evers, S., Yule, C.M., Padfield, R., O'Reilly, P., Keep, Varkkey H., 2017. Keep wetlands wet: the myth of sustainable development of tropical peatlands—implications for policies and management. *Glob. Chang. Biol.* 23 (2), 534–549.
- Forkuor, G., Dimobe, K., Serme, I., Tondoh, J.E., 2018. Landsat-8 vs. Sentinel-2: examining the added value of sentinel-2's red-edge bands to land-use and land-cover mapping in Burkina Faso. *GISci. Remote Sens.* 55 (3), 331–354.

- Friedlingstein, P., Jones, M., O'Sullivan, M., Andrew, R.M., Hauck, J., Peters, G.P., et al., 2019. Global carbon budget 2019. *Earth Syst. Sci. Data* 11 (4), 1783–1838.
- Frolking, S., Talbot, J., Jones, M.C., Treat, C.C., Kauffman, J.B., Tuittila, E.S., Roulet, N., 2011. Peatlands in the Earth's 21st century climate system. *Environ. Rev.* 19, 371–396.
- Gao, B.C., 1996. NDWI—a normalized difference water index for remote sensing of vegetation liquid water from space. *Remote Sens. Environ.* 58 (3), 257–266.
- GEE Data Catalogue, 2021. *Earth Engine Data Catalog, browse by dataset tags*. Available at <https://developers.google.com/earth-engine/datasets/tags>. (Accessed 30 April 2021).
- Gislason, P.O., Benediktsson, J.A., Sveinsson, J.R., 2006. Random forests for land cover classification. *Pattern Recogn. Lett.* 27 (4), 294–300.
- Global Carbon Project, 2020. *Global Carbon Budget 2020*. Available at <https://www.globalcarbonproject.org/carbonbudget/index.htm>. (Accessed 18 March 2021) (accessed 12 January 2021).
- Global Peatland Database, 2004. *Global Peatland Database of the International Mire Conservation Group*. Available at <https://www.greifswaldmoor.de/global-peatland-database-en.html>. (Accessed 2 May 2021).
- Goyder, D.J., Barker, N., Bester, S.P., Frisby, A., Janks, M., Gonçalves, F., 2018. The Cuito catchment of the Okavango system: a vascular plant checklist for the Angolan headwaters. *PhytoKeys* 11, 1–31.
- Grundling, P., Grootjans, A.P., 2016. Peatlands of Africa. *The Wetland Book*, pp. 1–10.
- Hategekimana, S., Twarabamenya, E., 2007. The impact of wetlands degradation on water resources management in Rwanda: the case of Rugezi Marsh. *Proceedings of the 5th International Symposium on Hydrology. Vol. 7*.
- Hogg, A.G., Heaton, T.J., Hua, Q., Palmer, J.G., Turney, C.S., Southon, J., et al., 2020. SHCal20 Southern Hemisphere calibration, 0–55,000 years cal BP. *Radiocarbon* 62 (4), 759–778.
- Huntley, B.J., Russo, V., Lages, F., Ferrand, N., 2019. *Biodiversity of Angola: Science & Conservation: A Modern Synthesis*. Springer Nature, pp. 25–30.
- Jaenicke, J., Rieley, J.O., Mott, C., Kimman, P., Siegert, F., 2008. Determination of the amount of carbon stored in Indonesian peatlands. *Geoderma* 147 (3–4), 151–158.
- Joosten, H., 2010. *The Global Peatland CO2 Picture: Peatland Status and Drainage Related Emissions in All Countries in the World. Report for Wetlands International, Waegeningen, The Netherlands*.
- Joosten, H., 2011. *Peatlands, policies and markets. Report to IUCN UK Peatland Programme, Edinburgh*. Available at www.iucn-uk-peatlandprogramme.org/scientificreviews. (Accessed 1 October 2021).

- Joosten, H., Clarke, D., 2002. Wise Use of Mires and Peatlands. International Mire Conservation Group and International Peat Society, p. 304.
- Kalacska, M., Arroyo-Mora, J.P., Soffer, R.J., Roulet, N.T., Moore, T.R., Humphreys, E., et al., 2018. Estimating peatland water table depth and net ecosystem exchange: a comparison between satellite and airborne imagery. *Remote Sens.* 10 (5), 687.
- Landis, J.R., Koch, G.G., 1977. An application of hierarchical kappa-type statistics in the assessment of majority agreement among multiple observers. *Biometrics* 33, 363–374.
- Lawson, I.T., Kelly, T.J., Aplin, P., Boom, A., Dargie, G., Draper, F.C., et al., 2015. Improving estimates of tropical peatland area, carbon storage, and greenhouse gas fluxes. *Wetl. Ecol. Manag.* 23 (3), 327–346.
- Lee, T.H., Ullah, A., Wang, R., 2020. *Bootstrap aggregating and random forest. Macroeconomic Forecasting in the Era of Big Data.* Springer, Cham, pp. 389–429.
- Lees, K.J., Quaife, T., Artz, R.R., Khomik, M., Clark, J.M., 2018. Potential for using remote sensing to estimate carbon fluxes across northern peatlands—a review. *Sci. Total Environ.* 615, 857–874.
- Limpens, J., Berendse, F., Blodau, C., Canadell, J.G., Freeman, C., Holden, J., et al., 2008. Peatlands and the carbon cycle: from local processes to global implications—a synthesis. *Biogeosciences* 5 (5), 1475–1491.
- Lindsay, R., 2010. *Peatbogs and Carbon: A Critical Synthesis to Inform Policy Development in Oceanic Peat Bog Conservation and Restoration in the Context of Climate Change. Report.* University of East London, Environmental Research Group.
- Loisel, J., Gallego-Sala, A.V., Amesbury, M.J., Magnan, G., Anshari, G., Beilman, D.W., et al., 2021. Expert assessment of future vulnerability of the global peatland carbon sink. *Nat. Clim. Chang.* 11 (1), 70–77.
- Mahdianpari, M., Salehi, B., Mohammadimanesh, F., Motagh, M., 2017. Random forest wetland classification using ALOS-2 L-band, RADARSAT-2 C-band, and TerraSAR-X imagery. *ISPRS J. Photogramm. Remote Sens.* 130, 13–31.
- Mahdianpari, M., Salehi, B., Mohammadimanesh, F., Homayouni, S., Gill, E., 2019. The first wetland inventory map of newfoundland at a spatial resolution of 10 m using sentinel-1 and sentinel-2 data on the google earth engine cloud computing platform. *Remote Sens.* 11 (1), 43.
- Marazzi, L., Gaiser, E.E., Jones, V.J., Tobias, F.A., Mackay, A.W., 2017. Algal richness and life-history strategies are influenced by hydrology and phosphorus in two major subtropical wetlands. *Freshw. Biol.* 62 (2), 274–290.
- McFeeters, S.K., 1996. The use of the Normalized Difference Water Index (NDWI) in the delineation of open water features. *Int. J. Remote Sens.* 17 (7), 1425–1432.

- McNemar, Q., 1947. Note on the sampling error of the difference between correlated proportions or percentages. *Psychometrika* 12 (2), 153–157.
- Midgley, J.M., Engelbrecht, I., 2019. New collection records for Theraphosidae (Aranea, Mygalomorphae) in Angola, with the description of a remarkable new species of *Ceratogyrus*. *Afr. Invertebr.* 60 (1), 1–13.
- Milzow, C., Kgotlhang, L., Bauer-Gottwein, P., Meier, P., Kinzelbach, W., 2009. Regional review: the hydrology of the Okavango Delta, Botswana—processes, data and modelling. *Hydrogeol. J.* 17 (6), 1297–1328.
- Minasny, B., Berglund, Ö., Connolly, J., Hedley, C., de Vries, F., Gimona, A., et al., 2019. Digital mapping of peatlands—a critical review. *Earth Sci. Rev.* 196, 102870.
- Minayeva, T.Y., Bragg, O., Sirin, A.A., 2017. Towards ecosystem-based restoration of peatland biodiversity. *Mires Peat* 19 (1), 1–36.
- Montanarella, L., Jones, R.J., Hiederer, R., 2006. Distribution of peatland in Europe. *Mires Peat* 1, 1–10.
- Mutanga, O., Kumar, L., 2019. Google Earth Engine applications. *Remote Sens.* 11 (5), 11–14.
- Myers, N., Mittermeier, R.A., Mittermeier, C.G., Da Fonseca, G.A., Kent, J., 2000. Biodiversity hotspots for conservation priorities. *Nature* 403 (6772), 853–858.
- Onojeghuo, A.O., Blackburn, G.A., Wang, Q., Atkinson, P.M., Kindred, D., Miao, Y., 2018. Mapping paddy rice fields by applying machine learning algorithms to multi-temporal Sentinel-1A and Landsat data. *Int. J. Remote Sens.* 39 (4), 1042–1067.
- Oon, A., Mohd Shafri, H.Z., Lechner, A.M., Azhar, B., 2019. Discriminating between large-scale oil palm plantations and smallholdings on tropical peatlands using vegetation indices and supervised classification of LANDSAT-8. *Int. J. Remote Sens.* 40 (19), 7312–7328.
- Page, S.E., Banks, C.J., Rieley, J.O., 2007. Tropical peatlands: distribution, extent and carbon storage-uncertainties and knowledge gaps. *Peatl. Int.* 2 (2), 26–27.
- Page, S.E., Rieley, J.O., Banks, C.J., 2011. Global and regional importance of the tropical peatland carbon pool. *Glob. Chang. Biol.* 17 (2), 798–818.
- Pajunen, H., 1996. *Peatlands in Burundi, Their Extent, Development and Use* (Finland).
- Ramsar, 2002. *Guidelines for Global Action on Peatlands from the Ramsar Convention*. Available at <https://www.ramsar.org/sites/default/files/documents/pdf/guide/guide-peatlands-e.pdf>. (Accessed 14 March 2021).
- Rieley, J., Page, S., 2016. *Tropical peatland of the world. Tropical Peatland Ecosystems*. Springer, Tokyo, pp. 3–32.

- Rodriguez-Galiano, V.F., Ghimire, B., Rogan, J., Chica-Olmo, M., Rigol-Sanchez, J.P., 2012. An assessment of the effectiveness of a random forest classifier for land-cover classification. *ISPRS J. Photogramm. Remote Sens.* 67, 93–104.
- Rouse, J.W., Haas, R.H., Schell, J.A., Deering, D.W., 1974. Monitoring vegetation systems in the Great Plains with ERTS. *NASA Special Publication.* 351, p. 309.
- Schefuß, E., Schouten, S., Schneider, R.R., 2005. Climatic controls on central African hydrology during the past 20,000 years. *Nature* 437 (7061), 1003–1006.
- Shanahan, T., McKay, N., Hughen, K., Overpeck, J.T., Otto-Bliesner, B., Heil, C.W., et al., 2015. The time-transgressive termination of the African Humid Period. *Nat. Geosci.* 8 (2), 140–144.
- Shier, C.W., 1985. Tropical peat resources—an overview. *Proceedings of Tropical peat resources—Prospects and Potentials Symposium, Kingston, Jamaica, February. International Peat Society, Helsinki*, pp. 29–46.
- Šimanauskienė, R., Linkevičienė, R., Bartold, M., Dąbrowska-Zielińska, K., Slavinskienė, G., Veteikis, D., Taminskas, J., 2019. Peatland degradation: the relationship between raised bog hydrology and normalized difference vegetation index. *Ecohydrology* 12 (8), e2159.
- Tanneberger, F., Moen, A., Joosten, H., Nilsen, N., 2017. The peatland map of Europe. *Mires Peat* 19, 1–17. <https://doi.org/10.19189/MaP.2016.OMB.264>.
- Taylor, P.J., Neef, G., Keith, M., Weier, S., Monadjem, A., Parker, D.M., 2018. Tapping into technology and the biodiversity informatics revolution: updated terrestrial mammal list of Angola, with new records from the Okavango Basin. *ZooKeys* 779, 51–88.
- Thanh Noi, P., Kappas, M., 2018. Comparison of random forest, k-nearest neighbor, and support vector machine classifiers for land cover classification using Sentinel-2 imagery. *Sensors* 18 (1), 18.
- Trettin, C.C., Labovitch, L., Lerotholi, S., Mercer, E., 2008. The peatlands of Lesotho—an important ecological and socio-economic resource. *After Wise Use-The Future of Peatlands.* 1, pp. 88–91.
- United States Geological Survey, 2020. *NDVI, The foundation for Remote Sensing Phenology*. Available at https://www.usgs.gov/core-science-systems/eros/phenology/science/ndvi-foundation-remote-sensing-phenology?qt-science_center_objects=0#qt-science_center_objects. (Accessed 30 October 2020).
- United States Geological Survey, 2021. *Landsat Surface Reflectance product overview*. Available at https://www.usgs.gov/core-science-systems/nli/landsat/landsat-surface-reflectance?qt-science_support_page_related_con=0#qt-science_support_page_related_con. (Accessed 20 January 2020).
- Wang, J., Rich, P.M., Price, K.P., Kettle, W.D., 2004. Relations between NDVI and tree productivity in the central Great Plains. *Int. J. Remote Sens.* 25 (16), 3127–3138.

Whyte, A., Ferentinos, K.P., Petropoulos, G.P., 2018. A new synergistic approach for monitoring wetlands using Sentinels-1 and 2 data with object-based machine learning algorithms. *Environ. Model Softw.* 104, 40–54.

World Wildlife Fund, 2021. *Miombo woodlands facts and figures*.

Available at

https://wwf.panda.org/discover/knowledge_hub/where_we_work/miombo_woodlands/.

(Accessed 10 May 2021).

Xu, J., Morris, P.J., Liu, J., Holden, J., 2018. PEATMAP: refining estimates of global peatland distribution based on a meta-analysis. *Catena* 160, 134–140.

Yurco, K., King, B., Young, K.R., Crews, K.A., 2017. Human–wildlife interactions and environmental dynamics in the Okavango Delta, Botswana. *Soc. Nat. Resour.* 30 (9), 1112–1126.

Zhang, W., Lu, Q., Song, K., Qin, G., Wang, Y., Wang, X., et al., 2014. Remotely sensing the ecological influences of ditches in Zoige Peatland, eastern Tibetan Plateau. *Int. J. Remote Sens.* 35 (13), 5186–5197.